



Synthesis and electrochemical properties of lithium nickel oxysulfide ($\text{LiNiS}_y\text{O}_{2-y}$) material for lithium secondary batteries

Sang Ho Park^a, Yang-Kook Sun^{a,*}, Ki Soo Park^b, Kee Suk Nahm^b, Yun Sung Lee^c, Masaki Yoshio^c

^a Department of Industrial Chemistry, College of Engineering, Hanyang University, Sungdong-Gu, 17 Haendang-Dong, Seoul 133-791, Republic of Korea

^b School of Chemical Engineering and Technology, College of Engineering, Chonbuk National University, Chonju 561-756, Republic of Korea

^c Department of Applied Chemistry, Saga University, 1 Honjo, Saga 840-8502, Japan

Received 1 October 2001; received in revised form 23 January 2002

Abstract

The layered oxysulfide $\text{LiNiS}_y\text{O}_{2-y}$ compounds were synthesized and characterized to investigate the effect of sulfur on the electrode performance of LiNiO_2 . LiNiO_2 precursors were first synthesized by a sol-gel method using adipic acid as a chelating agent and then doped with sulfur powders by a solid-state reaction under the flow of oxygen to prepare $\text{LiNiS}_y\text{O}_{2-y}$ compounds. Pure LiNiO_2 electrode showed a gradual decrease of discharge capacity with cycle number, whereas the capacity retention rate of $\text{LiNiS}_y\text{O}_{2-y}$ electrodes significantly improved. The initial discharge capacity of the $\text{LiNiS}_y\text{O}_{2-y}$ cells was lower than that of LiNiO_2 cell and decreased with the increasing content of sulfur substituted in $\text{LiNiS}_y\text{O}_{2-y}$. © 2002 Elsevier Science Ltd. All rights reserved.

Keywords: Nickel layered oxide; Anion substitution; Sol-gel chemistry; Electrochemical measurements; Lithium ion battery; Oxisulfide

1. Introduction

The layered lithium nickel oxide LiNiO_2 has been drawing much attention as a promising cathode material for lithium secondary batteries because of its comparatively low cost, large theoretical capacity (275 mAh/g), and environmental advantages over LiCoO_2 [1–3]. However, LiNiO_2 has still had some severe problems such as low discharge capacity (about 140–150 mAh/g) due to the difficulty in the synthesis of stoichiometric LiNiO_2 and capacity decay due to the formation of NiO_2 phase by the phase transition of LiNiO_2 structure during intercalation/deintercalation of lithium ion [4].

The synthesis of stoichiometric LiNiO_2 has been attempted by an excess lithium method in solid state reaction [5–7]. But this method has some difficulties in obtaining optimum composition because it requires washing process for removing excess lithium. Therefore,

many researchers have reported that the crystal structure of LiNiO_2 can be stabilized by substituting cation or anion of LiNiO_2 with the corresponding ions. Partial substitution of Ni for LiNiO_2 with some transition metals such as Al, Co, Ga, Mg, Ti, etc., has been widely studied to improve the cycle life of the electrode [8–12]. Also we reported that Al-doping LiNiO_2 cathode material was very effective in improving cycle performance at high temperature [13]. Meanwhile, Kubo et al. [14] and Naghash et al. [15,16] observed that the crystal structure of the material was stabilized by substituting O for LiNiO_2 with fluorine, resulting in the significant improvement of LiNiO_2 cyclability during intercalation/deintercalation of lithium ions. Recently, it was also found that anion doping with sulfur was very effective in stabilizing the crystal structure of LiMn_2O_4 [17,18].

In this work, we have synthesized $\text{LiNiS}_y\text{O}_{2-y}$ compounds and investigated the effect of S-doping on the electrochemical performance. $\text{LiNiS}_y\text{O}_{2-y}$ compounds were synthesized by partial substitution of oxygen for LiNiO_2 with sulfur. The structural and electrochemical properties of the synthesized materials

* Corresponding author. Tel.: +82-2-2290-0524; fax: +82-2-2282-7329.

E-mail address: shpark92@ihanyang.ac.kr (Y.-K. Sun).

were investigated using various analytical techniques. The effect of the amount of sulfur used in the synthesis of $\text{LiNiS}_y\text{O}_{2-y}$ compounds was examined to improve the LiNiO_2 electrode performance.

2. Experimental

$\text{LiNiS}_y\text{O}_{2-y}$ compounds were prepared as follows: LiNiO_2 gel precursor was first synthesized using a sol-gel method. Lithium acetate ($\text{Li}(\text{CH}_3\text{COO}) \cdot 2\text{H}_2\text{O}$) and nickel acetate ($\text{Ni}(\text{CH}_3\text{COO})_2 \cdot 4\text{H}_2\text{O}$) salts were used as starting materials for the synthesis of LiNiO_2 compounds. A stoichiometric amount of Li acetate ($\text{Li}(\text{CH}_3\text{COO}) \cdot 2\text{H}_2\text{O}$) and Ni acetate ($\text{Ni}(\text{CH}_3\text{COO})_2 \cdot 4\text{H}_2\text{O}$) salts (cationic ratio of $\text{Li}:\text{Ni} = 1:1$) was dissolved in deionised water. The dissolved solution was added into a continuously agitated aqueous adipic acid solution. Adipic acid was used as a chelating agent for the reaction. The molar ratio of adipic acid to total metal ions was fixed in unity. The prepared solution was evaporated at 70–80 °C for 5 h until a transparent sol was obtained. As water evaporates further, the sol turns into a viscous transparent gel. The prepared precursors were mixed with a stoichiometric amount of sulfur powders to have oxysulfide $\text{LiNiS}_y\text{O}_{2-y}$ ($y = 0, 0.1$, and 0.3) compositions. After the mixtures were sufficiently grinded, they were heated to 450 °C in a box furnace with a ramping rate of 1 °C/min and maintained at the temperature for 10 h to eliminate organic components. Thus precalcined mixtures were post-calcined at 750 °C in a flow of oxygen for 14 h. The cooling rate of the mixtures maintained 1 °C/min to prevent the cation mixing in LiNiO_2 .

After the synthesis, the amounts of Li, Ni, and S in the synthesized materials were analyzed with an inductively coupled plasma (ICP) and sulfur analyzer (LECO Co., CS 444), respectively, to determine the real chemical composition of the materials. The oxygen content was determined via mass balance. Powder X-ray diffraction (XRD, D/Max-3A, Rigaku) measurements using Cu-K α radiation were carried out to characterize the structural properties of the synthesized compounds. FTIR spectra were recorded on a Hartmann & Braun DA8 FT Spectrometer (BOMEM) in KBr pellets in the 3500–500 cm^{-1} range. The particle morphology of the compounds after the calcination was observed using a scanning electron microscope (SEM, GEOL, JSM 6400). Rietveld refinement was performed with XRD data to obtain lattice parameters of synthesized compounds.

The electrochemical characterization was performed using CR2032 coin-type cells. The method of assembling the cell was as follows: The cathode was fabricated with an accurately weighed active material (20 mg) and conductive binder (10 mg of Teflonized acetylene black

(TAB) and 5 mg graphite). It was pressed on 25 mm^2 stainless steel mesh used as the current collector at 300 kg/cm^2 and dried at 200 °C for 5 h in an oven. This cell consisted of a cathode and a lithium metal anode (Cyprus Foote Mineral Co.) separated by a porous polypropylene film as the separator (Celgard 3401). The electrolyte used was a 1 M LiPF_6 -ethylene carbonate (EC)/dimethyl carbonate (DMC) (1:2 by volume). The cell was assembled in an argon-filled dry box and tested at room temperature. The cell was charged and discharged at a current density of 0.4 mA/cm^2 (C/3) with cut-off voltages of 3.0–4.3 V(vs. Li/Li^+).

3. Results and discussion

Layered oxysulfide $\text{LiNiS}_y\text{O}_{2-y}$ materials ($y = 0, 0.1$, and 0.3) were prepared using sulfur powder to see the effect of sulfur content doped in the material on the electrode performance. Table 1 shows the real compositions of the synthesized LiNiO_2 , $\text{LiNiS}_{0.1}\text{O}_{1.9}$, and $\text{LiNiS}_{0.3}\text{O}_{1.7}$ compounds with their lattice constants. It was observed that the amount of actually doped sulfur was very small in $\text{LiNiS}_y\text{O}_{2-y}$ compounds.

Fig. 1 shows XRD patterns for the prepared samples. Fig. 1(a) is an XRD pattern for undoped LiNiO_2 , whereas Fig. 1(b) and (c) are XRD patterns for $\text{LiNiS}_y\text{O}_{2-y}$ ($y = 0.02, 0.03$) compounds, respectively. XRD spectra show that all the prepared samples have typical LiNiO_2 layered structure with a space group $R\bar{3}m$. No impurity peak is detected from the XRD spectra of LiNiO_2 and $\text{LiNiS}_{0.02}\text{O}_{1.98}$ compounds (Fig. 1(a) and (b)), whereas the XRD peak of LiOH impurity appears at $2\theta = 22^\circ$ from the $\text{LiNiS}_{0.03}\text{O}_{1.97}$ compounds although the magnitude of its inclusion is very low. All the peaks appeared from the XRD patterns were identified with the characteristic peaks of LiNiO_2 reported in the X-ray powder data file of JCPDS as well as previously reported works [4,19,20].

The lattice constants, a and c , of the synthesized materials were calculated by the Rietveld refinement using the XRD data of Fig. 1 and listed in Table 1. The lattice constants a and c were identified to remain almost constant about 2.88 and 14.19 Å, respectively, for all the prepared samples even though increasing the sulfur content in the material. This is because the amount of actually doped sulfur is very low in $\text{LiNiS}_y\text{O}_{2-y}$, as demonstrated in the chemical analysis. The previous works reported that the lattice constants of a and c of typical LiNiO_2 layered structure are 2.88 and 14.18 Å, respectively [4].

The electrochemical properties of LiNiO_2 have been estimated by measuring the integrated intensities of (003), (104), (006), and (101) peaks from XRD patterns [4,21]. The integrated intensities of (003), (104), (006), and (101) peaks were evaluated from the XRD patterns

Table 1
Lattice constants, lithium content, and sulfur content measured by Rietveld analysis, ICP, and sulfur analyzer, respectively

Nominal composition for $\text{LiNiS}_y\text{O}_{2-y}$	Lattice constants		Final Li composition (molar ratio)	Final S composition (molar ratio)
	a (Å)	c (Å)		
LiNiO_2	2.887	14.196	0.98	—
$\text{LiNiS}_{0.1}\text{O}_{1.9}$	2.880	14.199	1.01	0.02
$\text{LiNiS}_{0.3}\text{O}_{1.7}$	2.880	14.194	1.04	0.03

of Fig. 1 and the integrated intensity ratios of (003)/(104) and (006)/(101) peaks were depicted in the upper inset of Fig. 1. With increasing the sulfur content in the material, the intensity ratio of (003)/(104) peaks decreases from 1.5 to 1.12, whereas that of (006)/(101) peaks increases from 0.18 to 0.24. The previous work reported that the LiNiO_2 cathode material produces good electrochemical property when the intensity ratio of (003) and (104) peaks is higher than 1.2, while that of (006) and (101) peaks is lower than 1.0. Our observed data illuminate that the initial discharge capacity of our prepared samples will decrease with increasing sulfur content in the prepared samples.

The FTIR data collected on $\text{LiNiS}_y\text{O}_{2-y}$ ($y = 0.02$) powders generated by this process are shown in Fig. 2. The presence of sulfur bond could be confirmed by

observing the S–O vibration in the $\text{LiNiS}_y\text{O}_{2-y}$ ($y = 0.02$) powders. It should be mentioned that the S–O vibration attributed to the oxysulfide may not be easily identified in the FTIR analysis of the oxide powder. The characteristic S–O bands are strong stretch, which occurs in the range $1000\text{--}750\text{ cm}^{-1}$. Also, sulfur and oxide double bands occur at 1350 and 1175 cm^{-1} , respectively [22].

The morphology of the prepared samples was also observed with a SEM. Fig. 3(a) and (b) show SEM photographs for LiNiO_2 and $\text{LiNiS}_{0.02}\text{O}_{1.98}$ compounds, respectively. The shape of oxysulfide $\text{LiNiS}_{0.02}\text{O}_{1.98}$ is a little bit different from that of LiNiO_2 . The LiNiO_2 compound is shaped into a spherical structure, but the $\text{LiNiS}_{0.02}\text{O}_{1.98}$ shows a more rectangular shape. The average particle sizes of the powders are about $0.2\text{--}0.5$

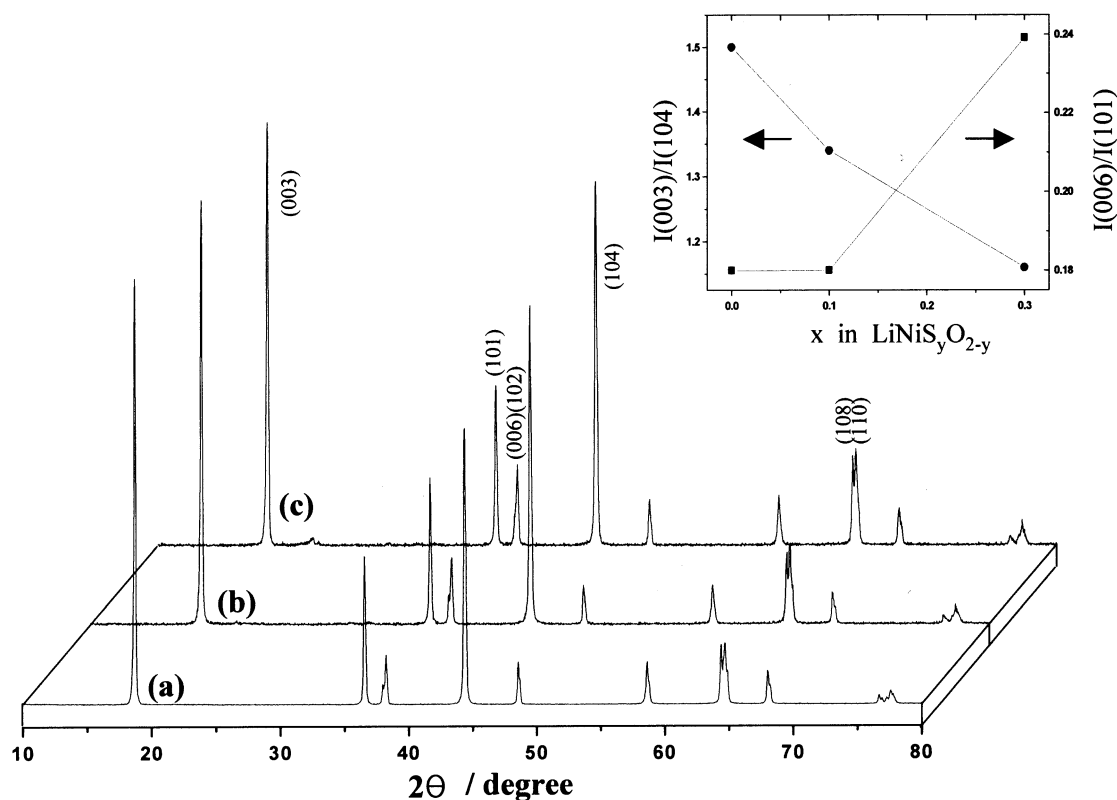


Fig. 1. X-ray diffraction patterns for (a) LiNiO_2 , (b) $\text{LiNiS}_{0.02}\text{O}_{1.98}$ and (c) $\text{LiNiS}_{0.3}\text{O}_{1.7}$ compounds prepared using sulfur powder at a pre-calcination temperature of 450°C . The gel precursors were calcined at 750°C in O_2 . The upper inset shows the integrated intensity ratios of $I(003)/I(104)$ and $I(006)/I(101)$ peaks as a function of sulfur content.

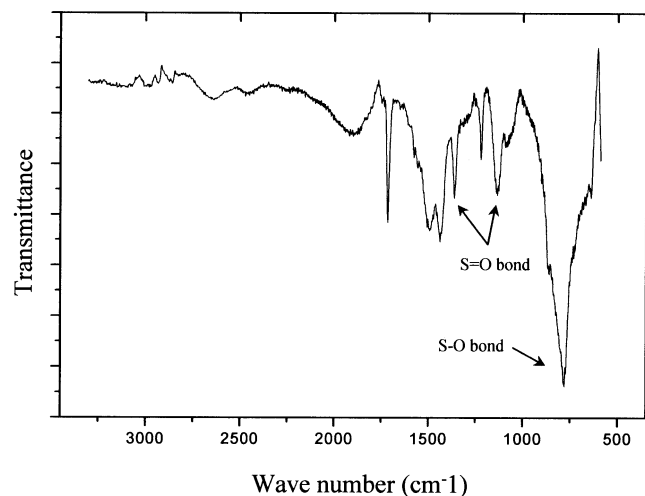


Fig. 2. FTIR spectroscopy (diffuse reflectance mode) measured from $\text{LiNiS}_{0.02}\text{O}_{1.98}$ powder.

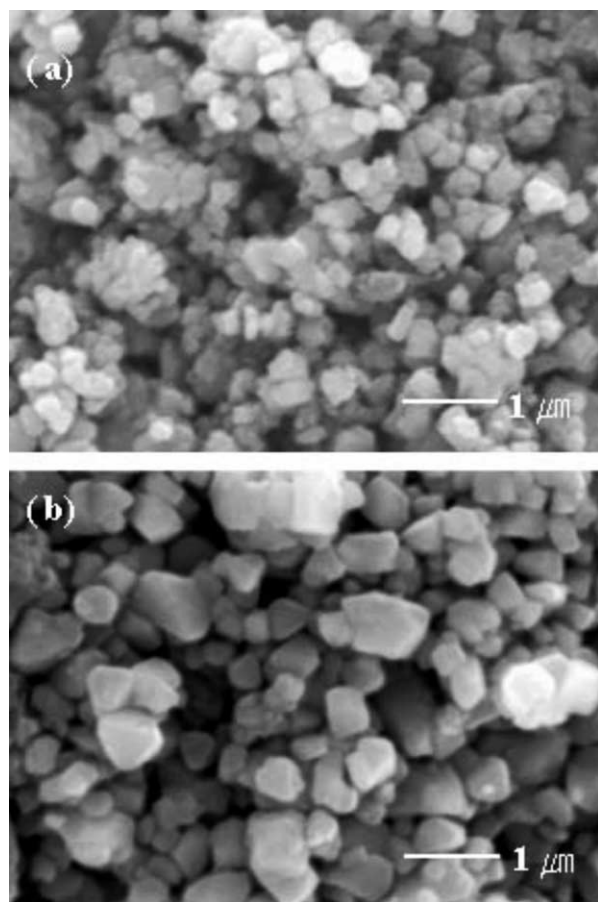


Fig. 3. Scanning electron micrographs for (a) LiNiO_2 and (b) $\text{LiNiS}_{0.02}\text{O}_{1.98}$.

μm for LiNiO_2 and $0.5\text{--}1\text{ }\mu\text{m}$ for $\text{LiNiS}_{0.02}\text{O}_{1.98}$, respectively. It is considered that the rectangular shape of the powders means that the $\text{LiNiS}_{0.02}\text{O}_{1.98}$ compounds have highly crystallized layered structure. At present, it seems that the structure of LiNiO_2 is strongly

stabilized by the S-doping. It was observed in our previous work that S-doped LiMn_2O_4 powder maintains its original structure even after several charge–discharge cycles [15,16].

Shown in Fig. 4 are plots of the discharge capacity measured at room temperature versus cycle number for the $\text{Li/LiPF}_6\text{-EC/DMC}$ (1:2 by vol.)/ $\text{LiNiS}_y\text{O}_{2-y}$ cells fabricated using the synthesized compounds. The cells were tested under a constant charge/discharge current density of 0.4 mA/cm^2 (C/3) between 3.0 and 4.3 V. Fig. 4(a) shows the discharge capacity for the cell fabricated with undoped LiNiO_2 compounds for comparison. The LiNiO_2 cell initially delivers a discharge capacity of 160 mAh/g. But the capacity gradually decreases with the cycle number to be 130 mAh/g after the 45th cycles. For the $\text{LiNiS}_{0.02}\text{O}_{1.98}$ and $\text{LiNiS}_{0.03}\text{O}_{1.97}$ cells, meanwhile, the capacity retention rates are significantly improved although the initial capacity of the cells decreases with the increase of sulfur content doped in $\text{LiNiS}_y\text{O}_{2-y}$. For example, $\text{LiNiS}_{0.02}\text{O}_{1.98}$ shows an initial discharge capacity of 140 mAh/g and has the discharge capacity of 130 mAh/g even after 85th cycle. This corresponds to 93% of the initial discharge capacity. The reduction of initial capacity by increasing S content in $\text{LiNiS}_y\text{O}_{2-y}$ compounds is due to the decrease of the amount of extractable lithium, as anticipated in the inset of Fig. 1. The removal of lithium from the layered nickel oxide is accompanied by an oxidation of Ni^{3+} to Ni^{4+} . In addition, the initial capacity of LiNiO_2 electrode varies depending on the amount of inserted/extracted Li^+ ions. In our experiments, it was found from the chemical analysis of the S-doped samples that the Li content increases with the increase of sulfur amount doped in $\text{LiNiS}_y\text{O}_{2-y}$. The inset of Fig. 1 showed the decrease of

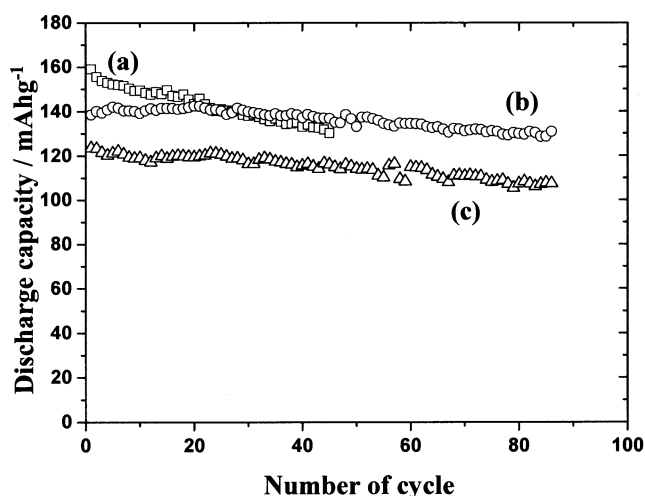


Fig. 4. Plots of specific discharge capacity vs. number of cycles for the $\text{Li/LiPF}_6\text{-EC/DMC}$ (vol.1:2)/ $\text{LiNiS}_y\text{O}_{2-y}$ powders. Cycling was carried out galvanostatically at constant charge/discharge current density of 0.4 mA/cm^2 between 3.0–4.3 V at room temperature. (a) LiNiO_2 , (b) $\text{LiNiS}_{0.02}\text{O}_{1.98}$, and (c) $\text{LiNiS}_{0.03}\text{O}_{1.97}$.

the integrated intensity ratio of the (003)/(104) peaks with the increase of sulfur content in $\text{LiNiS}_y\text{O}_{2-y}$. It is likely that the excess amount of lithium content slightly affects the degree of the displacement of lithium and nickel ions in the LiNiO_2 structure, resulting in the reduced initial capacity of $\text{Li}_{1+x}\text{NiO}_{2-y}\text{S}_y$.

Meanwhile, the capacity retention rate was apparently improved for the sulfur doped LiNiO_2 . At present, it is not clear why a better retention rate is attained from the sulfur doped lithium nickel oxides. But the following possibilities might be proposed to explain the improvement of the retention rate in the sulfur doped lithium nickel oxides. In S-doped layered NiO_2 framework, it is assumed that the partial substitution of oxygen with sulfur for LiNiO_2 might create a more flexible structure because the electronegativity of sulfur is lower than that of oxygen, which prevents the disintegration of the structure by the elongation between layers due to intercalation/deintercalation of lithium ions during the charge–discharge cycles. It also seems that this behavior is attributed to the increases of ion transport for lithium by the sulfur doping. According to the electrochemical study on thiospinel ($\text{Li}_x\text{Ti}_2\text{S}_4$) structure [23], it seemed reasonable to assume that the relatively large size and

polarizability of sulfur ions makes it easy for lithium ions to transport in the oxide structure, which reduces the structural strains of the material formed in the process of Li ion insertion. Another possibility might be assumed to be due to the catalytic activity of sulfur element in the synthetic process of S-doped LiNiO_2 phase. Some previous works reported the catalytic activity of sulfur in oxidation process of metals [24]. In Fig. 3, it was shown that the particle size of $\text{LiNiS}_{0.02}\text{O}_{1.98}$ is larger than that of LiNiO_2 . This suggests that the sulfur might act as a catalyst in the synthetic process of S-doped LiNiO_2 to increase the particle size and enhance the structural stability. Consequently, it seems that the substitution of a small amount of S for O stabilizes the structural integrity of the electrode material which in turn increases the electrode performance.

The stabilization of the LiNiO_2 structure might be indirectly explained from the charge–discharge curves of cells. Fig. 5(a) and (b) show the charge–discharge curves for LiNiO_2 and $\text{LiNiS}_{0.02}\text{O}_{1.98}$ cells, respectively. The charge–discharge curve of LiNiO_2 (Fig. 5(a)) has four distinct plateaus in the whole cut-off voltage region. The plot agrees well with results published in the literature, which show four-stepped structural changes in the charge process [14,25]. The appearance of the potential plateau near 4.0 V Li/Li^+ is due to the formation of NiO_2 phase, which causes the capacity fade

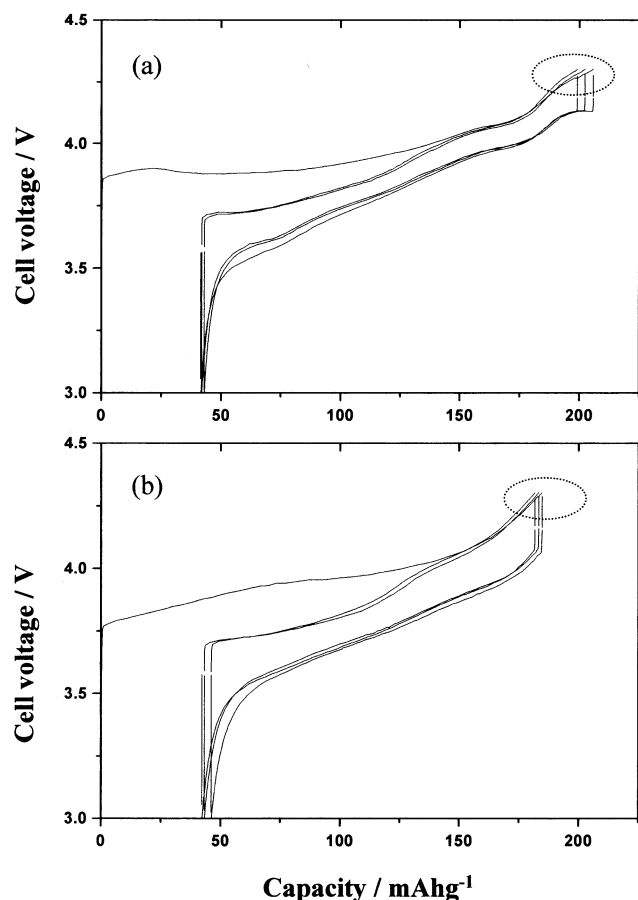


Fig. 5. Charge–discharge curves for (a) LiNiO_2 and (b) $\text{LiNiS}_{0.02}\text{O}_{1.98}$ measured at room temperature.

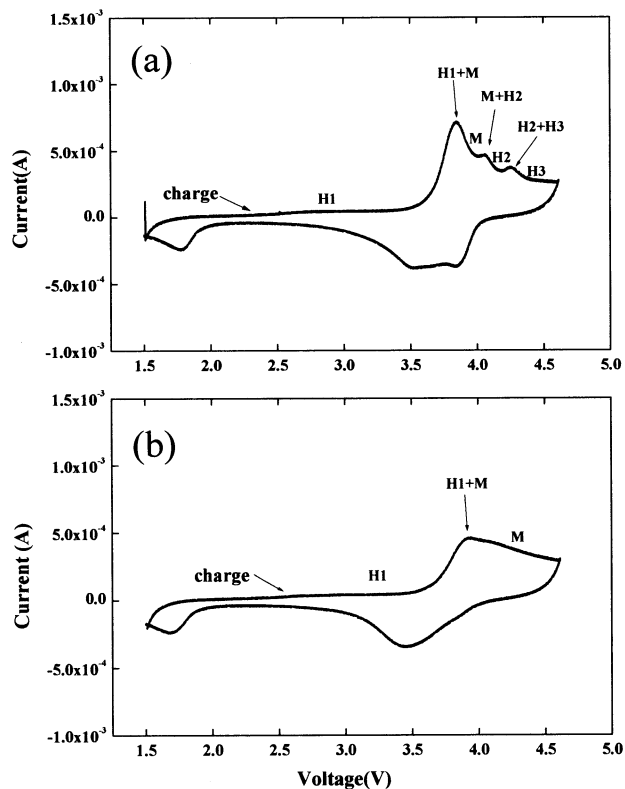


Fig. 6. Cyclic voltammograms for (a) LiNiO_2 and (b) $\text{LiNiS}_{0.02}\text{O}_{1.98}$ measured at 0.2 mV/s.

of the LiNiO_2 electrode during cycling. However, the charge–discharge curve of the $\text{LiNiS}_{0.02}\text{O}_{1.98}$ cell (Fig. 5(b)) is different from that of LiNiO_2 (Fig. 5(a)). The plateau is not observed in the charge–discharge curve of $\text{LiNiS}_{0.02}\text{O}_{1.98}$. The observation of a monotonous curve in the charge voltage region indicates that no phase transition occurs during cycling and lithium ion diffusion can proceed in a single phase.

We also measured the cyclic voltammograms of LiNiO_2 and $\text{LiNiS}_{0.02}\text{O}_{1.98}$ and showed them in Fig. 6(a) and (b), respectively. In Fig. 6(a), three peaks appear from the charge curve measured at the second cycle. The peaks represent the occurrence of electrochemical reactions due to the phase changes of LiNiO_2 during cycling. In the charging process, it was reported that LiNiO_2 showed a sequential change in the crystal structure from the hexagonal phase (H1) to the monoclinic phase (M), hexagonal phase (H2) again, then two hexagonal phases (H2+H3), finally a single hexagonal phase (H3) [25]. They suggested that these phase changes are related to the deformation of the NiO_2 layer in the LiNiO_2 crystal lattice, resulting in an irreversible structure change. However, no peak is observed from the charge curve of $\text{LiNiS}_{0.02}\text{O}_{1.98}$ measured at the second cycle, as shown in Fig. 6(b). The monotonous variation of the charge curve evidences that there is no phase transition during the charge–discharge processes. This indicates that the S-doping greatly improves the stability of the LiNiO_2 structure and retains its original layered structure during the charge–discharge processes. Consequently, the above two electrochemical measurements clearly demonstrate that the structure of LiNiO_2 can be significantly stabilized by the S-doping, producing the fact that the cyclability of $\text{LiNiS}_y\text{O}_{2-y}$ ($y = 0.02$ and 0.03) is superior to that of LiNiO_2 .

4. Conclusions

We have synthesized and characterized layered oxy-sulfide $\text{LiNiS}_y\text{O}_{2-y}$ compounds to develop good cathode material for the secondary lithium batteries. The structural and electrochemical characteristics of the prepared $\text{LiNiS}_y\text{O}_{2-y}$ powders were investigated as a function of the content of sulfur doped in $\text{LiNiS}_y\text{O}_{2-y}$ compounds. The LiNiO_2 cell initially delivers a discharge capacity of 160 mAh/g. But the capacity gradually decreases with the cycle number. For the $\text{LiNiS}_y\text{O}_{2-y}$ ($y = 0.02, 0.03$) cells, the capacity retention rates are significantly improved. But the initial capacity

of the cells decreases with the increases of sulfur content doped in the material.

Acknowledgements

The authors wish to acknowledge the financial support of the Korea Research Foundation made in the program year of 2000.

References

- [1] C. Delmas, *Mater. Sci. Eng. B3* (1989) 97.
- [2] A.F. Wells, *Structural Inorganic Chemistry*, Oxford Science Publications, 1975, p. 577.
- [3] J.N. Reimers, W. Li, E. Rossen, J.R. Dahn, in: *MRS Symp. Proc.*, Vol. 293, G.A. Nazri, J.M. Tarascon, M. Armand (Eds.), Pittsburgh, 1993, p. 3.
- [4] T. Ohzuku, A. Ueda, M. Nagayama, *J. Electrochem. Soc.* 140 (1993) 1563.
- [5] H. Arai, S. Okada, H. Ohtsuka, M. Ichimura, J. Yamaki, *Solid State Ionics* 80 (1995) 261.
- [6] H. Arai, S. Okada, Y. Sakurai, J. Yamaki, *J. Electrochem. Soc.* 144 (1997) 3117.
- [7] H. Arai, S. Okada, Y. Sakurai, J. Yamaki, *Solid State Ionics* 109 (1998) 295.
- [8] T. Ohzuku, T. Yanagawa, M. Kouguchi, A. Ueda, *J. Power Sources* 68 (1997) 131.
- [9] Y. Nitta, K. Okamura, K. Haraguchi, S. Kobayashi, A. Ohta, *J. Power Sources* 54 (1995) 511.
- [10] B. Banov, J. Bourilkov, M. Mladenov, *J. Power Sources* 54 (1995) 268.
- [11] Y. Nishida, K. Nakane, T. Satoh, *J. Power Sources* 68 (1997) 561.
- [12] H. Arai, S. Okada, Y. Sakurai, J. Yamaki, *J. Electrochem. Soc.* 144 (1997) 3117.
- [13] S.H. Park, K.S. Park, Y.K. Sun, K.S. Nahm, Y.S. Lee, M. Yoshio, *Electrochim. Acta* 46 (2001) 1215.
- [14] K. Kubo, M. Fujiwara, S. Yamada, S. Arai, *J. Power Sources* 68 (1997) 553.
- [15] A.R. Naghash, J.Y. Lee, *Electrochim. Acta* 46 (2001) 2293.
- [16] A.R. Naghash, J.Y. Lee, *Electrochim. Acta* 46 (2001) 941.
- [17] S.H. Park, K.S. Park, Y.K. Sun, K.S. Nahm, *J. Electrochem. Soc.* 147 (2000) 2116.
- [18] Y.K. Sun, B.K. Oh, H.J. Lee, *Electrochim. Acta* 46 (2000) 541.
- [19] S. Yamada, M. Fujiwara, M. Kanda, *J. Power Sources* 54 (1995) 209.
- [20] A. Rougier, P. Grovereau, C. Delmas, *J. Electrochem. Soc.* 143 (1996) 1168.
- [21] Y. Nitta, K. Okamura, K. Haraguchi, S. Kobayashi, A. Ohta, *J. Power Source* 54 (1995) 511.
- [22] D.L. Pavia, G.M. Lampman, G.S. Kriz, *Introduction to Spectroscopy*, 2nd ed., Department of Chemistry, Western Washington University, Bellingham, WA, 1996.
- [23] J.B. Goodenough, *Solid State Ionics* 69 (1994) 184.
- [24] D. Fatcasiu, J.Q. Li, S. Cameron, *Appl. Catal.* 154 (1997) 173.
- [25] T. Ohzuku, A. Ueda, M. Nagayama, *J. Electrochem. Soc.* 140 (1993) 1862.